資料番号：27－１

# MONJU Core Neutronics Analysis Method Upgrading Research

## – New Collapsing Algorithm for Condensation of the Transport Cross-Sections for the 3-D Transport Code NSHEX –

**Galina TODOROVA　　Hiroshi NISHI　　Junichi ISHIBASHI**

International Cooperation and Technology Development Center, Tsuruga Head Office

## 「もんじゅ」炉心核特性解析手法の高度化研究
## －３次元輸送計算コードNSHEXにおける新たな輸送断面積縮約手法開発－

ガリーナ・トドロヴァ　　西　　裕士　　石橋　淳一

敦賀本部　国際技術センター

*The 3-D transport discrete-ordinate code NSHEX has been implemented for solving a range of criticality problems concerning FBR MONJU. In order to reduce the existing energy-group collapsing effect in the few-group results for the effective multiplication factor (keff), a new algorithm for condensation of the macroscopic transport cross-section (XS) has been proposed. This paper overviews the recent progress of MONJU criticality analysis and presents a description on the new collapsing algorithm, the results from verification tests and a discussion from the viewpoint of the finite-difference method of the code NSHEX. According to the presented results, the new collapsing algorithm reduces the energy-group collapsing effect for keff and improves the fast flux space distribution. It can be recommended as a better algorithm for condensation of the transport XS for the code NSHEX instead of the conventional current-weighted method.*

３次元ノード法Sn輸送計算コードNSHEXによる輸送効果補正評価では，少数群縮約断面積を用いた場合，エネルギー群縮約効果が無視できなかった。このNSHEXコードにおける輸送断面積の扱いについて，筆者らはその原因がノード内の中性子束分布を関数近似していることにあることを明確化し，これに基づく輸送断面積の新たな縮約手法を提案した。本稿では，まず「もんじゅ」炉心の臨界性解析に関する最新の知見を概観し，それとの関係を含めて上記輸送断面積の新たな縮約手法につき紹介する。「もんじゅ」炉心の臨界性解析については，これまでにも各種検討が実施されている。その中で，輸送効果補正は重要な因子のひとつであるが，この手法によれば実効増倍係数の群縮約依存性が解消できるだけでなく，中性子の空間分布についても改善が見られることを，参照解に基づく検証計算により明確化した。これより，本縮約手法が従来手法に替えて推奨できることを確認した。

*Key Word*

*FBR, MONJU, Criticality Analysis, Transport Cross-Section, Energy-Group Collapsing, Nodal Method, Transport Code, Discrete-Ordinate Method,NSHEX, JENDL-3.2*

**キーワード**

**FBR,「もんじゅ」, 臨界性解析, 輸送断面積, エネルギー群縮約, ノード法, 輸送計算コード, 角度分点法, NSHEX, JENDL-3.2**

**ガリーナ・トドロヴァ※**

炉心技術開発グループ所属
日本学術振興会外国人特別研究員
ブルガリア・ヴァルナ工科大学講師，炉物理専攻
工学博士

**西　　裕士**

炉心技術開発グループ所属
グループリーダー
「もんじゅ」，FBRの炉心特性解析・遮蔽設計解析及びその高度化研究に従事

**石橋　淳一**

炉心技術開発グループ所属
「もんじゅ」の炉心解析及びその高度化研究に従事

※現在：ヴァルナ自由大学助教授
Associate Professor,Varna Free University

## 1. Introduction

The initial criticality of the Japanese prototype FBR MONJU was achieved in April 1994. The major reactor core characteristics were measured and analyzed by criticality experiments and physics analysis[1), 2)] using the JUPITER analysis system[3)].

The criticality of the FBR core, like MONJU, should be analyzed exactly based on the transport equation of the neutrons without any finite difference approximations of the neutron energy and space coordinate or geometry approximation. This kind of exact analytical calculation is becoming practical due to the recent progress in computer technology, using the continuous energy Monte-Carlo method. However, this method demands huge amount of computer resources and the obtained results contain certain statistical errors. Therefore, it is still important to improve and to validate the accuracy of the conventional deterministic method.

This paper overviews the recent progress in the MONJU criticality analysis and presents some new findings concerning the transport effect correction discussed in detail later.

## 2. Overview of Recent Progress

Recently the advanced core analysis system MEISTER has been developed[4)] and utilized for MONJU core physics test analysis. MEISTER system is being developed aiming at an interactive overall core characteristics analysis tool for use on a PC in an easy but accurate manner. Some examples of input and output screens are shown in Figures 1 and 2. MEISTER system assumes 24 mesh per assembly and 18 energy group calculation as the standard option, instead of the conventional 6 mesh per assembly and 7 energy group calculation.

But the MEISTER system has been established based on the conventional diffusion approximation calculation instead of the exact transport calculation, assuming the isotropic scattering of the neutrons in the core as usually assumed. The transport correction by the application of the exact three-dimensional (3D) hexagonal transport code, like NSHEX[5)], is one of the major issues to be investigated for the accurate physics analysis of the MONJU core.

Moreover, it is common that the neutron energy is divided into finite number of energy groups and the space coordinate is approximated

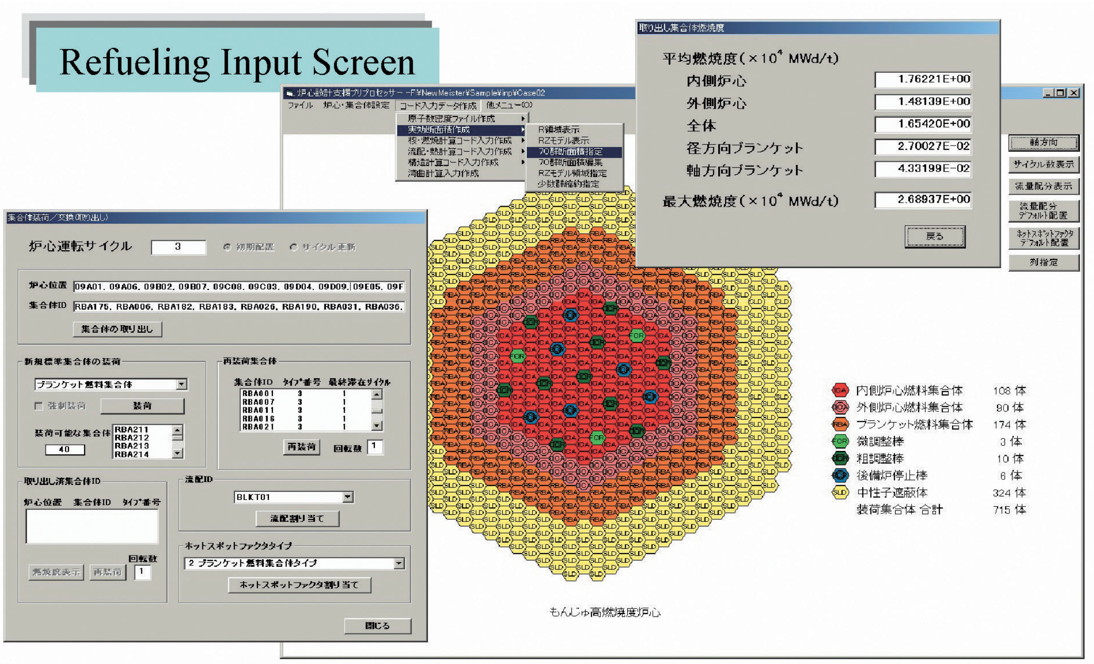


**Fig. 1 MEISTER System Pre-processor (An Example of Input Screen)**

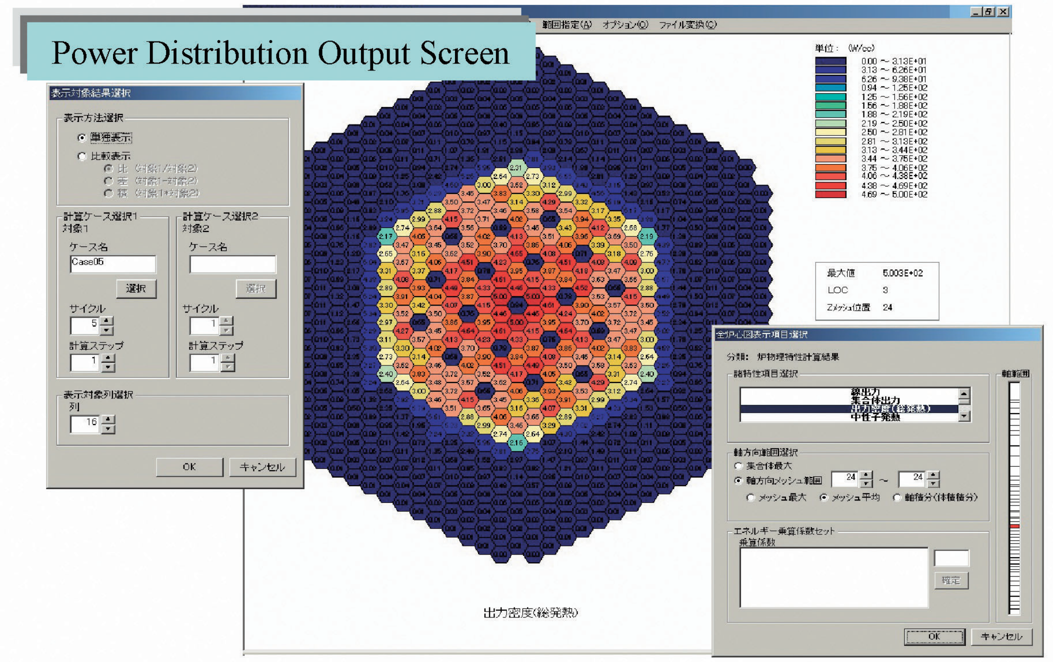


**Fig. 2　MEISTER System Post-processor (An Example of Output Screen)**

by finite-size mesh interval in order to enable the numerical calculation by the computers. The fine internal structure of the fuel assembly: fuel pellet, cladding, wrapper tube, etc., is usually approximated into homogenized model. These approximations require the correspondent corrections to obtain the exact final results.

These corrections are usually evaluated by comparing the obtained results of the approximated method and the exact method assuming a typical core model. As a result, these corrections for the criticality analysis of the MONJU initial critical core were evaluated as follows, for example, depending on the reference approximation methods [3), 6)]:

(1) Transport effect: +0.5 to +0.6% $\Delta k_{eff}$

(2) Cell heterogeneity effect: +0.4 to +0.6% $\Delta k_{eff}$

(3) Energy group collapsing effect: <0.1% $\Delta k_{eff}$

(4) Mesh effect: -0.1% $\Delta k_{eff}$

Most recent evaluation results of these corrections are shown in Figure 3. The basic result was based on the MEISTER calculation with 24 mesh per assembly and 18 energy group option. The mesh effect was evaluated by comparing the results by the fine mesh calculations based on the inversed mesh-squared rule. The neutron energy group collapsing effect was evaluated by comparing the results of Monte-Carlo calculations with different energy group structures, e.g. 70 energy group and continuous energy. The transport effect was examined with the homogeneous cell model calculations, where the continuous energy Monte-Carlo method was compared to the MEISTER diffusion method with corrections for the mesh and energy group effects. Then the cell heterogeneity effect was evaluated by the exact heterogeneous Monte-Carlo calculation.

The final corrected exact results were compared with the measured data and the E (Experiment)/ C (Calculation) correction was applied to adjust the bias of the used nuclear data library based on the past critical experiments or MONJU measured data. An example of the excess reactivity prediction for the MONJU initial start-up core, not only by the E/C correction method but also by the nuclear data library adjustment method, is shown in Figure 4. These results show some discrepancy between the E/C correction method and the adjusted library method, which should be investigated further. One of the possible reasons for this is that these evaluations are based on the probabilistic: Monte-Carlo method. Therefore, the evaluation by the conventional deterministic

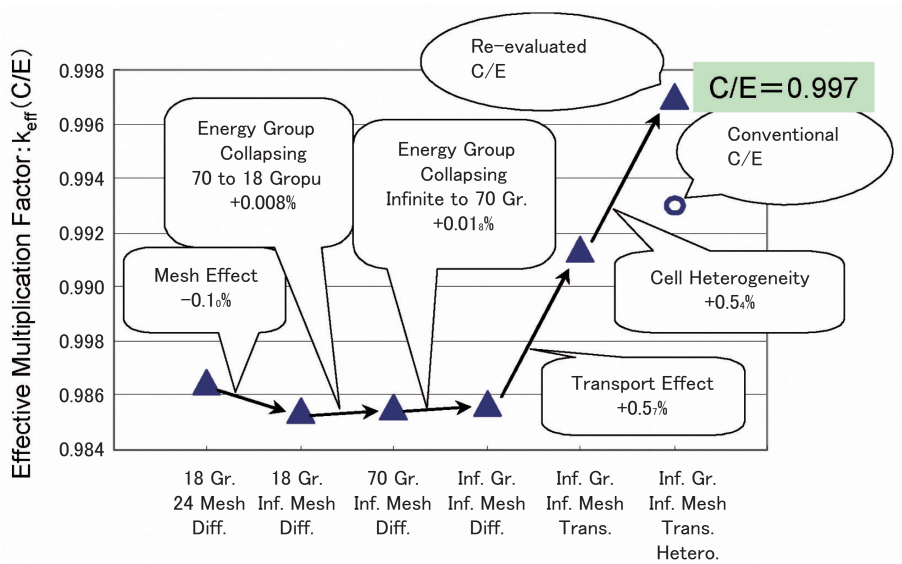


**Fig. 3 Corrections for Criticality Analysis by Homogeneous Diffusion Calculation**

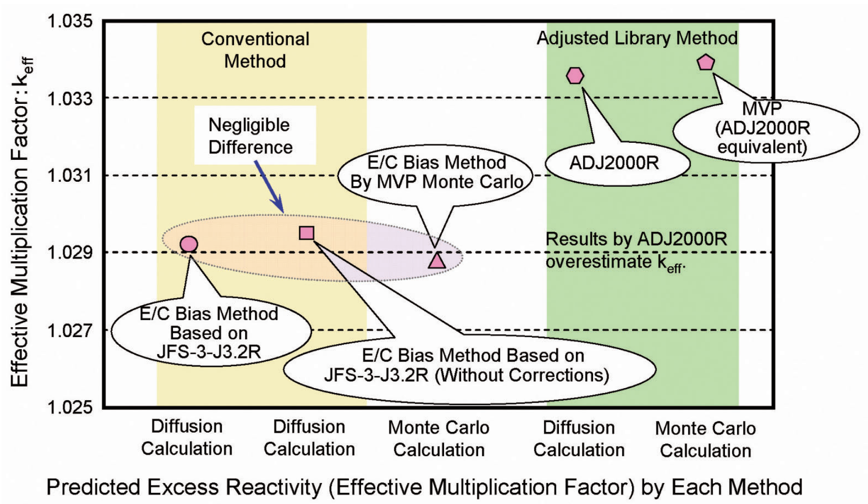


**Fig.4 MONJU Initial Start-up Core Excess Reactivity Prediction**

method would be helpful in improving prediction accuracy. The transport effect evaluation by the exact deterministic three-dimensional (3D) hexagonal transport code NSHEX was conducted for the accurate physics analysis of the MONJU core.

### 3. Transport Effect Evaluation by NSHEX

The code NSHEX is a hexagonal geometry 3D transport code that solves the neutron transport problem by a discrete-ordinate nodal method, which gives consistent results with the most recent CEA's reactor analysis system ERANOS[7] results (below 0.04% $\Delta k_{eff}$ difference) by the non-collapsed 70 energy-group calculations. The anisotropic scattering effect is simulated by the extended transport approximation. The neutron transport equation is solved using a nodal scheme with one mesh cell (node) per hexagonal assembly in plane. The node-internal spatial neutron flux distribution and transverse leakage distribution are simulated using second order polynomial-series approximation. Advanced methods for accurate description of radial and axial neutron leakage are incorporated into the code[8), 9)]. These methods have been verified by NEA/CRP 3D Neutron Transport Benchmark Model and large assembly-size KNK-II Model[10].

It is well known that the transport methods in core-physics analysis demand huge computational resources: CPU time and computer processing memory. The application of these methods is therefore limited and are applied mainly to the evaluation of the transport effect corrections for the diffusion results. Such kind of analysis was usually performed for problems of smaller size and coarse energy-group approximation, for example, 2D R-Z model or small 3D X-Y-Z model with 7 energy-group approximation, assuming the inter-independency of the transport effect correction from the energy-group approximation or from the core modeling. As the size of the problem depends on the core model, energy-group approximation and the method-associated approximation, the 3D transport code NSHEX has been utilized mainly by low-order discrete-ordinate approximation ($S_4$) and up to 18 energy-group approximation in partial-core models for MONJU criticality analysis.

The authors presented the results from discrete-ordinate analysis by the code NSHEX for a wider range of 3D core models. As a result, a good agreement between NSHEX and the Monte-Carlo probabilistic code GMVP[11] was pointed out. The maximal differences were below 0.1% $\Delta k_{eff}$, as a confirmation for the applicability of the code NSHEX to the MONJU whole core analysis in 70 energy-group calculations. However, the large energy group collapsing effect of NSHEX, which was not found in the GMVP results, remained as a major issue to be investigated further[12, 13, 14]. For example, the effect of the energy-group collapsing from 70 to 18 groups had been evaluated by the diffusion code system MEISTER to be at the order of 0.01% $\Delta k_{eff}$[6]. The NSHEX transport results, however, showed the effect to be more than several scores of times larger.

Current core design considers 1% $\Delta k_{eff}$ of the design margin for the core reactivity (effective multiplication factor) as shown in the safety analysis report for licensing. To increase the accuracy of the prediction and to decrease the current design margin leads to improved design method for the future up-graded MONJU core (for instance, even 0.1% $\Delta k_{eff}$ reduction of the uncertainty allows for 6 days extension of full-power operation). This is schematically shown in Figure 5.

The MONJU whole core analysis in 70 energy-group calculation obliges some limit in the Sn-order approximation, even when using the most recent computer such as the engineering workstation. This requires the elimination of such a large energy-group approximation dependency for the practical application of the deterministic transport method. A proposal of a new condensation algorithm for the transport XS in few energy-group structures has been developed recently, that has

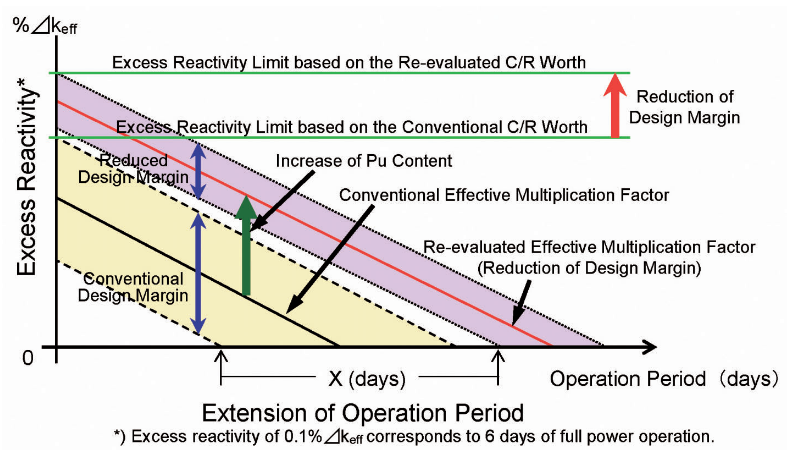


**Fig. 5 Extension of Operation Period by Design Margin Reduction**

been verified by a number of 3D MONJU simulation tests[15), 16)]. The details of the proposed method are shown below.

## 4. Solved problems and used methods

### 4.1. MONJU cores

FBR MONJU is a sodium-cooled MOX fueled ($PuO_2$-$UO_2$) reactor with thermal power of 714 MW. The reactor core consists of two plutonium enrichment zones (inner and outer core) of different Pu/(Pu+U) weight ratio (Figure 6). The plutonium-enriched zones are surrounded by radial and axial (upper and lower) blankets, which contain depleted $UO_2$ fuel. Axial and radial shields for reduction of the neutron fluence on the core internals and the reactor vessel surround all the fissile and fertile fuel zones. Two MONJU cores of different core layout have been analyzed: the initial critical core (ICC) (Figure 7) and the initial start-up core (ISC) (Figure 8). The ICC corresponds to the FBR MONJU core layout when the initial criticality has been achieved while the ISC corresponds to the core layout at the beginning of the initial operation cycle of the FBR MONJU as a power plant. One important feature of the ICC is that 30 fuel sub-assemblies in the outer core are replaced by dummy fuels. In addition to the ICC and ISC whole core models, a series of simplified models have also been simulated (ICC1, ICC2, ICC3) that consider simplified core configurations as follows: in the model ICC1 the radial blanket and the radial shield are ignored; in the model ICC2 the axial shields are also removed in addition to ICC1; the model ICC3 considers only the plutonium-enriched zones. The discrete-ordinate analysis by the code NSHEX has been performed in S4 approximation under convergence criteria of $5\times10^{-5}$ for $k_{eff}$ and $5\times10^{-4}$ for the neutron flux.

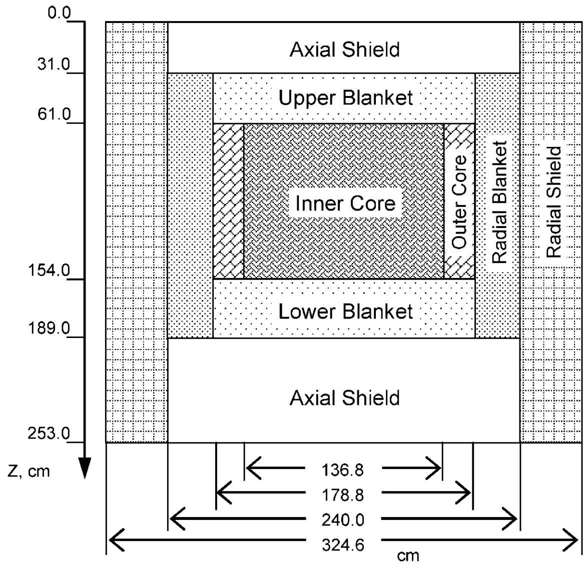


**Fig. 6 FBR MONJU R-Z scheme**

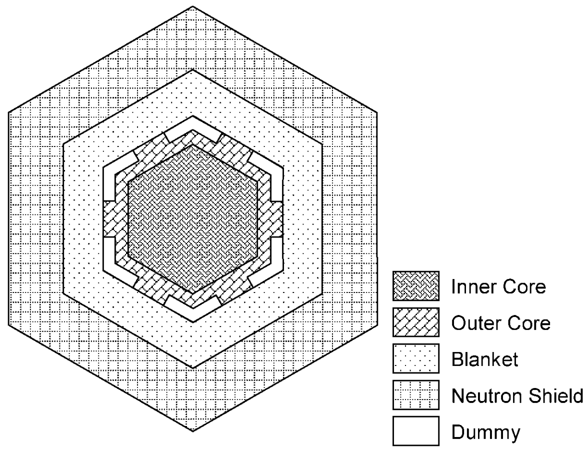


**Fig. 7 MONJU ICC layout**

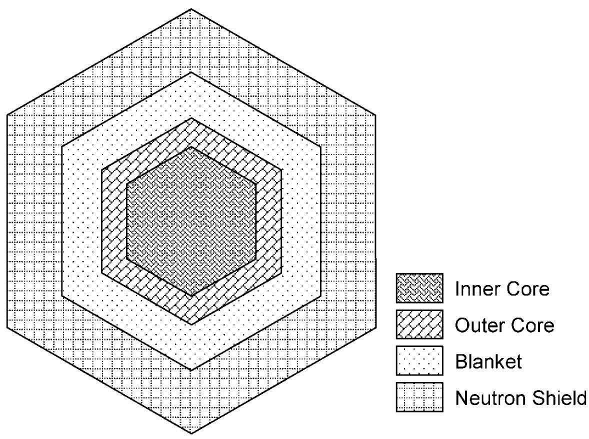


**Fig. 8 MONJU ISC layout**

### 4.2. XS preparation

In this study the macroscopic XS in 70 energy-group structure have been deduced from the derived 70 energy-group grouped constant set for fast reactors JFS-3-J3.2R based on the Japanese evaluated nuclear data library JENDL-3.2[17)] by the code SLAROM[18)]. These XS have been used in the 70 energy-group criticality analyses of the MONJU cores. For the few energy-group analyses, the XS have been condensed by the code JOINT[19] using the 70 energy-group fluxes calculated by the 2D R-Z option of the diffusion code CITATION[20]. The transport XS have been condensed by two methods: the conventional current-weighted method

$$\Sigma_{tr,G} = \frac{\sum_{g\in G} \Sigma_{tr,g} D_g \Phi_g}{\sum_{g\in G} D_g \Phi_g}, \text{ where } D_g = 1/3\Sigma_{tr,g} \tag{1}$$

and by the new collapsing algorithm, defined bellow.

### 4.3. Definition of the new collapsing algorithm

The new algorithm for condensation of $\Sigma_{tr}$ can be represented in a standard formulation as

$$\Sigma_{tr,G} = \sum_{g\in G} \Sigma_{tr,g} F_g , \tag{2}$$

where the weighting functions $F_g$ are defined as

$$F_g = \Sigma^{\gamma}_{tr,g}\Phi_g / \sum_{g\in G} \Sigma^{\gamma}_{tr,g}\Phi_g , \tag{3}$$

considering $\gamma$ =-1/2:

$$F_g = (\Phi_g / \sqrt{\Sigma^{g}_{tr,g}}) / \sum_{g\in G} (\Phi_g / \sqrt{\Sigma_{tr,g}}) \tag{4}$$

Both flux-weighted and current-weighted methods can be commonly described by the equation (3) where the different power coefficients represent the different collapsing methods: $\gamma$=0 for the flux-weighed method, while $\gamma$=-1 for the current-weighted method. The new collapsing algorithm therefore is proposed in the same general formulation of the weighting functions, however, the new $\gamma$ represents another correlation between the collapsing fluxes and the transport XS in the weighting functions. For simplicity, the new collapsing algorithm will be noted bellow as CCM (Combined Collapsing Method), as it can be formally considered as a combination between the flux-weighted and the current-weighted methods.

## 5. Results

### 5.1. The transport XS

The transport XS in 18 energy-group structure, obtained by the current-weighted collapsing and present method (CCM) have been compared. It has been found that the new collapsing algorithm (CCM) causes an increase of the transport XS, which is most significant in the energy groups 6 (from 0.821 MeV to 0.388 MeV) and 13 (from 4.31 keV to 2.03 keV). Figure 9 presents the percentage rise of $\Sigma_{tr}$ for the inner-core material composition of the MONJU ICC due to the new collapsing algorithm. In the two above-mentioned energy groups, the transport XS change has been evaluated to be 1.69% and 3.55%, respectively.

An additional preliminary study has been performed in order to evaluate the sensitivity of the ef-

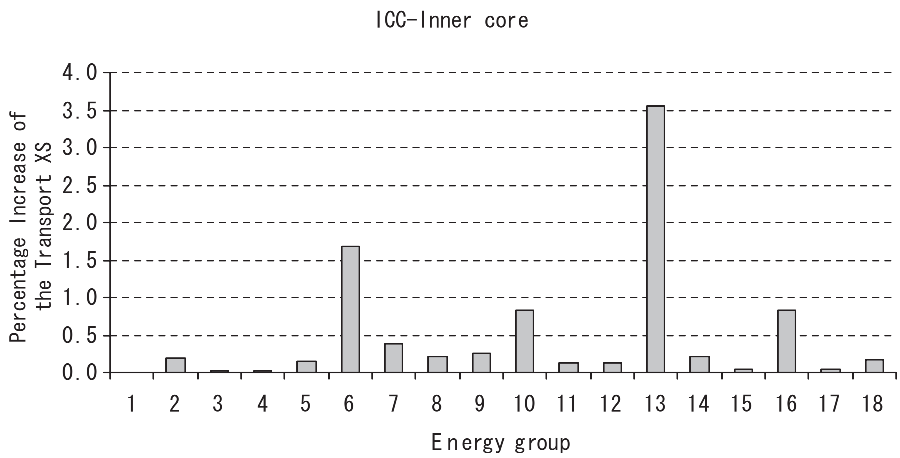


**Fig. 9 Percentage increase of the transport XS due to the present collapsing method**

fective multiplication factor to the macroscopic effective transport XS in the different energy groups. The quantities $S_{\Sigma_{tr},g} = \delta k_{eff} / \delta\Sigma_{tr,g}$ (the percentage change of $k_{eff}$, caused by 1% rise of the transport XS in the given energy group) have been calculated varying the transport XS in the inner-core and outer-core of MONJU ICC. Figure 10 shows the results for $S_{\Sigma_{tr},g}$ that have been obtained by NSHEX calculations in $S_4$ approximation. It can be noticed that the sensitivity coefficients are very small in the low-energy region. This implies that the significant rise of the transport XS in the energy group 13 due to the new collapsing method actually has negligibly small effect on the $k_{eff}$, while the increased transport XS in the energy-group 6 may cause more notable effect. The values of the transport XS in 70 and 18 energy-group structures, obtained for the interval of energies, corresponding to the energy-group 6 are presented in Figure 11, where the collapsing fluxes are shown as well.

### 5.2. The energy-group approximation effect of $k_{eff}$

First of all the results from 70 energy-group NSHEX analyses have been verified. The percentage differences $\Delta k_{eff} = (k_{eff}^{NSHEX} - k_{eff}^{ref}) / k_{eff}^{ref} * 100$

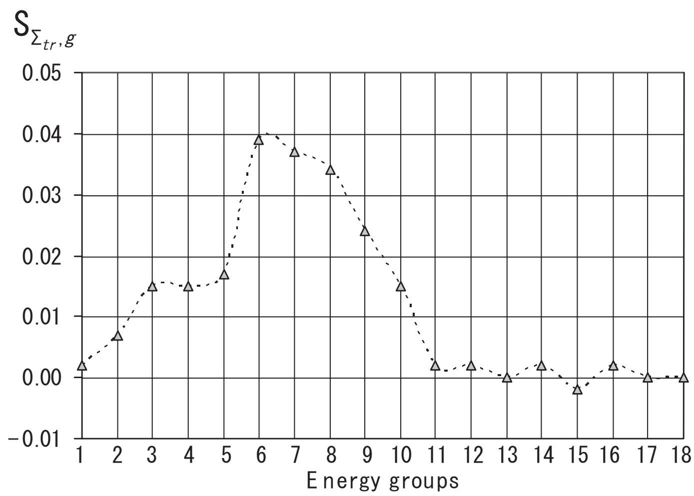


**Fig. 10 Sensitivity of the $k_{eff}$ to the macroscopic transport XS**

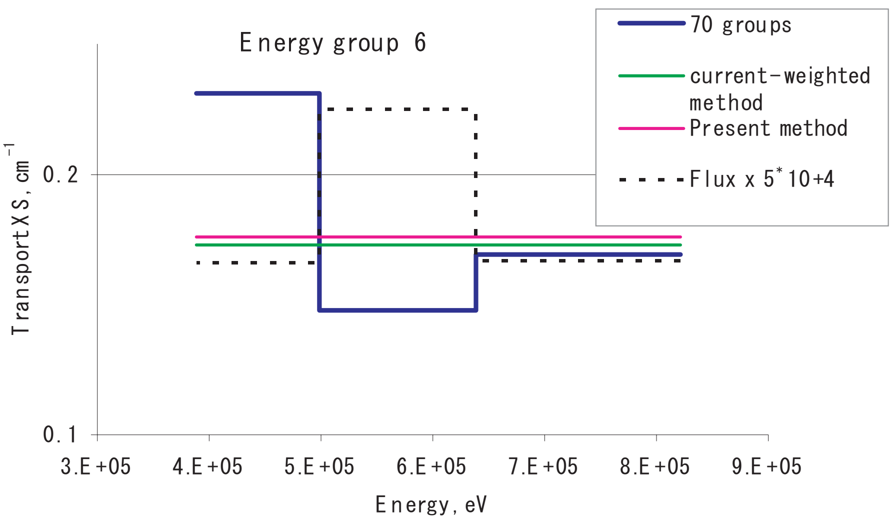


**Fig. 11 The transport XS, collapsed in 18 energy-group structure by the current-weighted and the present methods — Inner core, ICC**

are shown in Table 1, where the GMVP or ERANOS results are considered as reference. These results show very good agreement between the NSHEX and the transport deterministic and probabilistic results in 70 energy-group approximations. The few-energy-group criticality analyses for the above-mentioned MONJU cores have been conducted with XS that have been prepared using the current-weighted collapsing method and then applying the new CCM. The energy-group collapsing effect has been estimated comparing $k_{eff}$ from the few-group analysis with the corresponding 70 energy-group values: $(k_{eff}^{G} - k_{eff}^{70}) / k_{eff}^{70} * 100$ . The results are shown in Table 2 as well as Figures 12 and 13.

**Table 1. Verification of 70 energy-group NSHEX results for $k_{eff}$**

| Case | Reference code | % $\Delta k_{eff}$ |
|---|---|---|
| ICC | GMVP | -0.03 |
| ISC | GMVP | -0.10 |
| ISC | ERANOS | -0.04 |

**Table 2. The energy-group collapsing effect, $\%\Delta k_{eff} / k_{eff}^{70}$**

| Energy-group approximation | 18 groups | | 7 groups | |
|---|---|---|---|---|
| Collapsing Method | Current-weighted | CCM | Current-weighted | CCM |
| ICC | -0.12 | -0.001 | -0.19 | -0.003 |
| ICC1 | -0.12 | -0.08 | -0.33 | -0.10 |
| ICC2 | -0.20 | -0.05 | -0.31 | -0.09 |
| ICC3 | -0.19 | -0.02 | -0.32 | -0.03 |
| ISC | -0.15 | -0.05 | -0.25 | -0.09 |

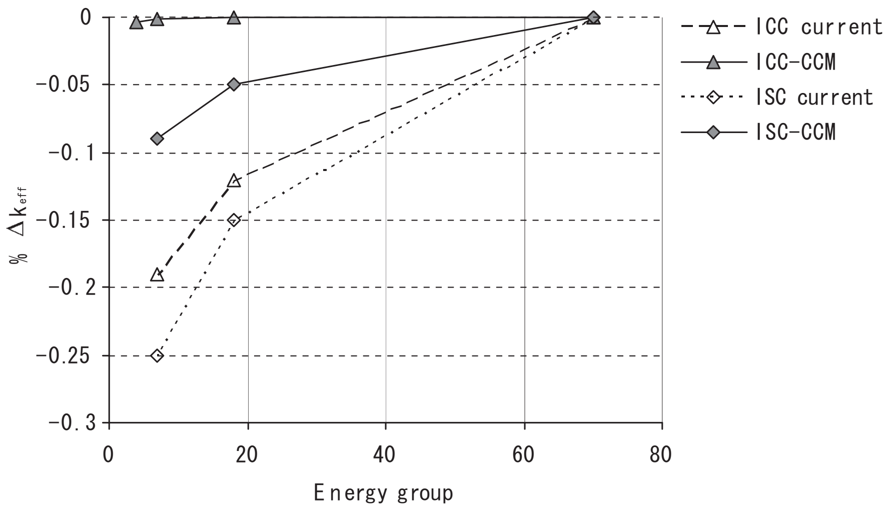


**Fig. 12 The energy-group collapsing effect for the whole-core tests**

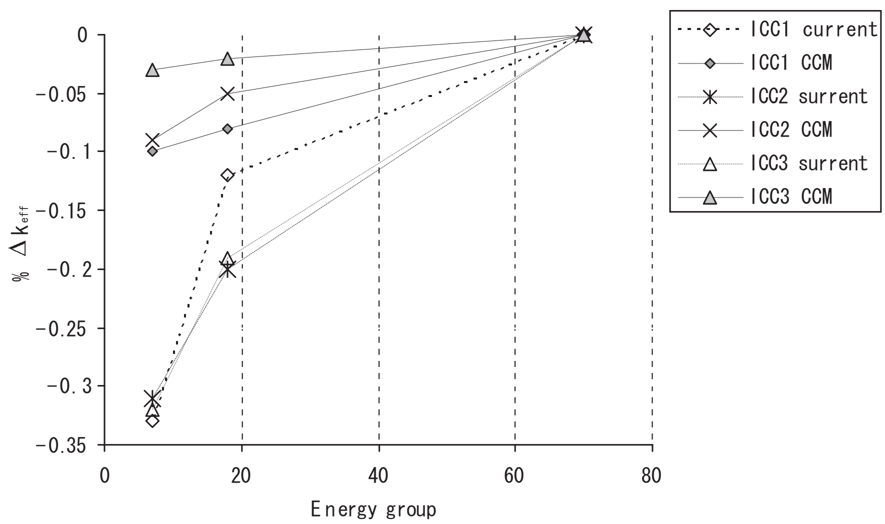


**Fig. 13 The energy-group collapsing effect for the simplified-core tests**

There are two things that are to be emphasized: in all test results the energy-group collapsing effect is significantly reduced in case the CCM is applied; in case of the CCM no any remarkable dependency exists of the energy-group collapsing effect from the core models, while in the case of the current-weighted collapsing method, the energy-group collapsing effect is larger for the simplified-core model tests.

### 5.3. Fast flux space distribution

For the purposes of numerical analyses of the space and energy distributions of the neutron fluxes, a new software module based on the Mathematica-5 software has been developed. This module has been applied as a supportive tool to analyze and visualize the numerical results from the NSHEX calculations. In this study the energy of 0.086 MeV has been considered as the low-energy border of the analyzed flux that will be noted conditionally as fast flux. This is because the bottom limit of the fast energy region of 0.1 MeV cannot include the whole 8-th energy group in the 18-group structure.

The 3D distribution of the fast flux has been analyzed for the ISC test in 70 and 18 energy-group approximations. The fast fluxes, calculated for each node in 18 energy-group approximation, have been compared with the corresponding fast fluxes from the 70 energy-group calculations. Figure 14 presents the relative differences where the 70-group data have been considered as reference.

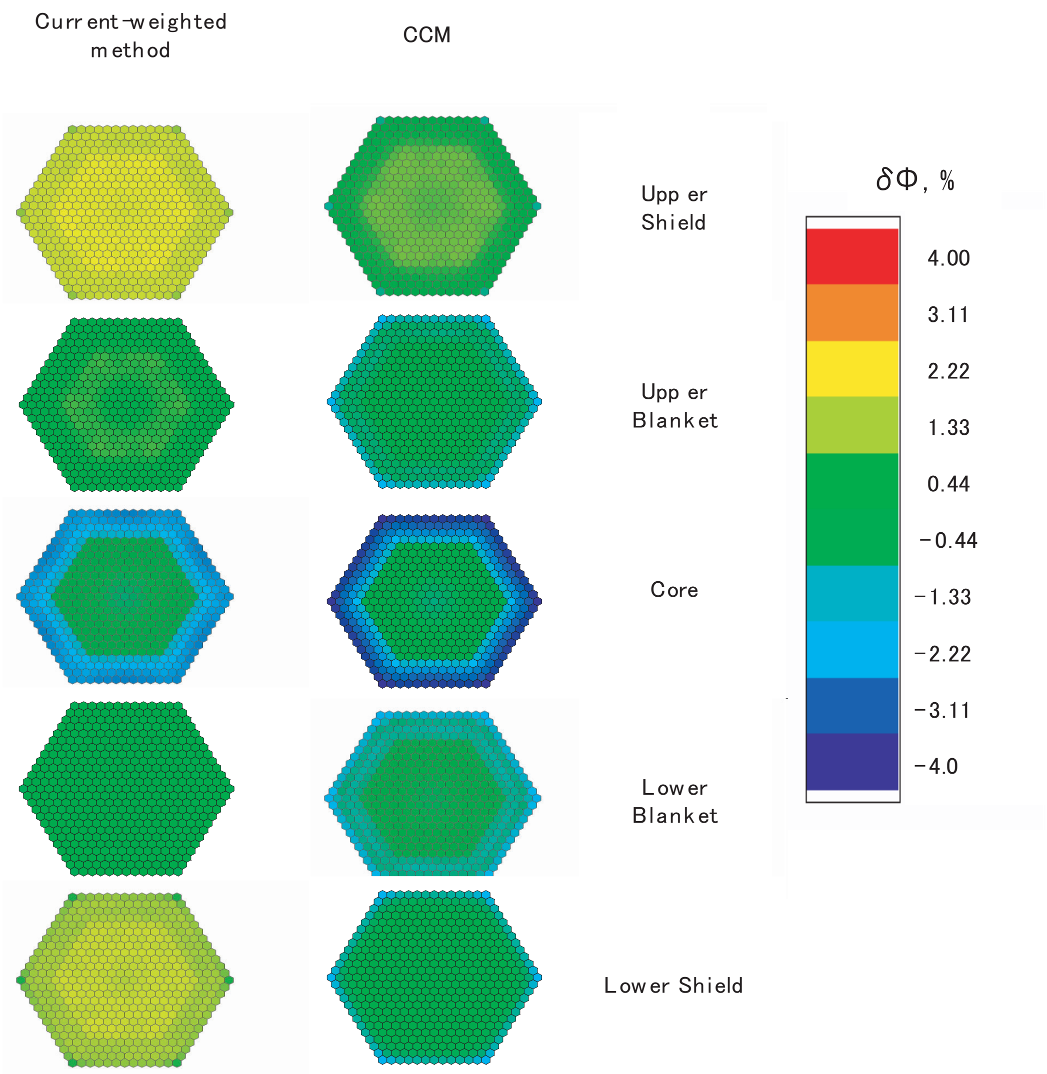


**Fig. 14 Comparison between the fast fluxes in 70 and 18 energy-group results**

The two series correspond to the results that have been obtained applying different collapsing methods for the transport XS in the 18 energy-group analyses. The pictures in the series visualize the above-mentioned percentage differences in the nodes positioned at about the middle of the corresponding axial regions.

The results from the comparisons show that in both cases (current-weighed method and CCM) the fast flux data in 18 energy-group approximation are in very good agreement with the 70 energy-group data for the inner core and outer core, where the differences are below 0.5%. Some underestimation of the fast flux can be noticed in radial blanket and radial shield for both series (slightly stronger in the case of CCM) that indicated for underestimated neutron leakage from these nodes in 18-groups analyses. The most notable difference between the two series is the upper and lower shields. By the current-weighted method the fast flux in the axial shields is overestimated in the 18 energy group analyses up to 2 % while by the CCM results are in very good agreement with the 70 energy-group data.

Figure 15 shows the percentage differences for the fast neutron flux, averaged over all nodes in plane. It can be noticed that the averaged fast flux in the 18 energy-group approximation is somewhat overestimated in the axial blankets and axial shields, but by the CCM the overestimation is reduced to below 1% and it is about two times smaller than that of the current-weighted method.

## 6. Discussion

All numerical results indicate that the CCM can provide better transport XS condensation than the current-weighted method. As it has been mentioned above, the energy group collapsing effect (by the current-weighted collapsing method) is more significant for simulation tests with increased neutron leakage. It has been presumed that transport XS collapsing by the current-weighted collapsing method causes overestimation of the neutron leakage. In contrast with the current-weighted method, the CCM produces a negligibly small energy-group collapsing effect that is almost independent from the core models. This implies that the new collapsing algorithm contributes to the better description of the neutron leakage in the few-group analysis.

While the flux-weighted method preserves the reaction rates in the few energy-group structure, the current-weighted method aims at preserving the neutron mean free path $\lambda_{tr,g}$ multiplied by the flux $\Phi_g$[21]:

$$\lambda_{tr,G} = \frac{\sum_{g\in G}\lambda_{tr,g}\Phi_g}{\sum_{g\in G}\Phi_g} = \frac{\sum_{g\in G} D_g\Phi_g}{\sum_{g\in G}\Sigma_{tr,G} D_g \Phi_g} = \frac{1}{\Sigma_{tr,G}}$$

The common understanding that the neutron cur-

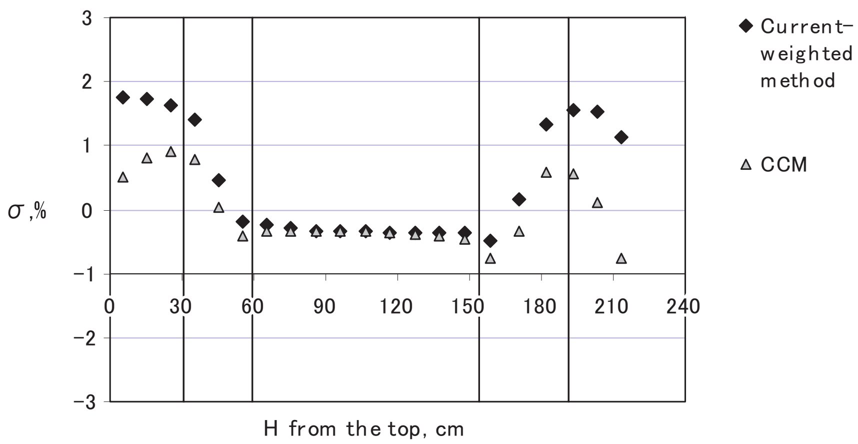


**Fig. 15 Percentage differences between 18 and 70 energy-group averaged fast fluxes - axial distribution**

rent has to be preserved is based on the Fick's law $J=-D\ grad\Phi$ that is often used in the numerical description of the neutron leakage. The XS condensation with preserving the neutron current is applied under the assumption that flux gradients have the same energy dependency like the scalar fluxes. In fact, the best method for condensation of $\Sigma_{tr}$ is the method, which is consistent with the physics model for simulation of the neutron leakage in the code. The nodal-equivalent finite-difference (NEFD)[5] method, which is incorporated in the code NSHEX, applies a higher-order algorithm in the simulation of the integral neutron leakage from each node. In order to clarify the dependency of the neutron leakage on the transport XS condensation, a short description of the NEFD is necessary.

In a multi-group formulation, the 3D $S_n$ neutron transport equation for energy group $g$ is described as follows:

$$\Omega^m \cdot \nabla \Psi_g{}^m(x,y,z) + \Sigma_{tr,g}\Psi_g{}^m(x,y,z) = Q_g(x,y,z) \quad (5)$$

where the following notations are used:

$\Omega^m$ - Vector of the m-th angular direction;

$\Psi_g^m(x, y, z)$ - Angular flux in the m-th angular direction;

$\Sigma_{rt,g}$ - Transport macroscopic effective cross-section, corrected against the scattering anisotropy;

$Q_g(x, y, z)$ - the fission and scattering source that is considered to be isotropic and is determined via the macroscopic fission and scattering XS and the scalar flux $\Phi_g(x, y, z)$.

The code NSHEX solves the 3D problem by a set of one-dimensional problems, found from (5) by double transverse integration (for example over axes y and z):

$$\frac{\mu_x^m}{h_r}\cdot\frac{\partial}{\partial x}[y_s(x)\Psi^m(x)] + \Sigma_{tr}y_s(x)\Psi^m(x) = y_s(x)Q(x) - L_\perp^m(x), \quad (6)$$

where $\mu_x^m$ is the x- component of the neutron flight path in the m-direction ($\eta^m$ and $\xi^m$ correspond to y and z); $y_s(x) = (1-|x|)/\sqrt{3}$ is the function that represents the x-dependency of the y-coordinates of the hexagonal node's boundaries in plane; $h_r$ - the horizontal mesh spacing; $L_\perp^m(x)$ is the transverse leakage term. The suffix for energy group "g" is omitted for simplicity. The hexagonal geometry is considered in a coordinate system {$\underline{x}$, z} ($\underline{x}$ = x, u, v) where the axes are perpendicular to the walls of the hexagonal node. The averaged dimensional angular fluxes $\Psi_0^{\underline{x},m}$ are assumed equal to the nodal averaged angular flux $\Psi_0^m$ that is computed from the 3D neutron balance equation. The total leakage per unit volume is represented by:

$$L^m = \frac{2}{3h_r}[\mu_x^m(\Psi_{x+}^{m,out} - \Psi_{x-}^{m,in}) + \mu_u^m(\Psi_{u+}^{m,out} - \Psi_{u-}^{m,in}) + \mu_v^m(\Psi_{v+}^{m,out} - \Psi_{v-}^{m,in})] + \frac{\xi^m}{h_z}(\Psi_{z+}^{m,out} - \Psi_{z-}^{m,in}), \quad (7)$$

where $\Psi_{x-}^{m,in}$ and $\Psi_{x-}^{m,out}$ are the surface-averaged angular fluxes on the left- and the right-sides of each node, known as the in-coming ($\Psi_{x-}^{m,in}$) and the out-going ($\Psi_{x-}^{m,out}$) angular fluxes. The nodal coupling equations that relate the in-coming and out-going angular fluxes are derived from the analytic solution of Eq. (6). This analytic solution can be numerically computed if the functions $Q(x)$ and $L_\perp^m(x)$ are approximated. The NEFD method assumes second-order polynomials approximation for $\Psi^m(x)$, $\Phi(x)$, $Q(x)$ and $L_\perp(x)$:

$$\Psi^m(x) = \sum_{i=0}^{2}\Psi_{i,x}^m h_i\ ; \qquad h_i = (1, x, x^2 - 5/72) \quad (8)$$

$$\Phi(x) = \sum_{i=0}^{2}\Phi_{i,x}h_i$$

$$Q(x) = \sum_{i=0}^{2}Q_{i,x}h_i$$

$$L_\perp(x) = \begin{cases} L_{r+}^{x,m}(x>0) \\ L_{r-}^{x,m}(x<0) \end{cases} + y_s(x)\sum_{i=0}^{2}L_{z,i}^{x,m}h_i\ ,$$

where $L_{r,+}^{x,m}$ and $L_{r,-}^{x,m}$ are the radial parts of the transverse leakage that correspond to x>0 and x<0 and $L_{z,i}^{x,m}$ are the moments of the axial part of the transverse leakage. The scalar flux moments $\Phi_{i,x}$ are computed via the angular flux moments $\Psi_{i,x}^m$ by quadrature and then are used for computation of the source moments $Q_{i,x}$. In the calculation of the transverse leakage moments, both the scalar flux moments and the angular flux moments are used[9].

In the NEFD method the following high-order relations between the in-coming and the out-going angular fluxes are derived for description of the dimensional neutron leakage:

$$\Psi_{x+}^{m,out} = \Psi_{x-}^{m,in} + \frac{\Psi_0^m - (\beta_x^m \Psi_{x-}^{m,in} + \delta_x^m)}{\alpha_x^m}$$
$$\Psi_{z+}^{m,out} = \Psi_{z-}^{m,in} + \frac{\Psi_0^m - (\beta_z^m \Psi_{x-}^{m,in} + \delta_z^m)}{\alpha_z^m} , \quad (9)$$

where $\delta_x^m$ and $\delta_z^m$ represent the intra-node increment of the m-th neutron angular flux along the x and z axis and the coefficients { $\alpha_x^m$, $\beta_x^m$ } and { $\alpha_z^m$, $\beta_z^m$ } are calculated via the response-matrix coefficients $F_0^{x,m}$, $G_{00}^{x,m}$, $\varepsilon_x^m$, $F_0^{z,m}$, $G_{00}^{z,m}$, $\varepsilon_z^m$ :

$$\alpha_x^m = \frac{G_{00}^{x,m}}{F_0^{x,m}}, \qquad \alpha_z^m = \frac{G_{00}^{z,m}}{F_0^{z,m}}$$
$$\beta_x^m = \frac{G_{00}^{x,m} + G_0^{x,m} F_0^{x,m} - G_{00}^{x,m}\varepsilon_x^m}{F_0^{x,m}} \quad (10)$$

$$\beta_z^m = \frac{G_{00}^{z,m} + G_0^{z,m} F_0^{z,m} - G_{00}^{z,m}\varepsilon_z^m}{F_0^{z,m}} = 1 \quad (11)$$

$$\varepsilon_x^m = \exp(-\frac{\Sigma_{tr} h_r}{\mu_x^m}), \qquad \varepsilon_z^m = \exp(-\frac{\Sigma_{tr} h_z}{\xi^m}) \quad (12)$$

From Eq. (7) and Eq. (9) it is easy to notice that the quantities that multiply the angular fluxes in the simulation of the neutron leakages are $\frac{1}{\alpha_k^m}$ and $\frac{\beta_k^m}{\alpha_k^m}$ for $k$=$x$, $u$, $v$, $z$. Assuming that the angular fluxes have the same energy dependency like the node-averaged scalar flux, it can be concluded that the dimensional leakages would be effectively preserved in a few energy-group structure, if the XS collapsing is performed by a method that can preserve $\frac{\Phi_g}{\alpha_k^m}$ , taking into account that $0 < \beta_k^m \leqq 1$. In this study the functions $\frac{1}{\alpha_x^m}$ have been computed from Eq. (10). The expressions for the response-matrix coefficients have been derived by substituting the polynomials (7) in the analytic solution of the Eq. (6) and applying the weighted-residual method as in Ikeda's paper[5]. As a result, the following expressions have been found, that represent the dependency of $F_0^{x,m}$ and $G_{00}^{x,m}$ on $\Sigma_{tr}$ :

$$F_0^{x,m} = \frac{\exp(\frac{-h_r\Sigma_{tr}}{\mu_x^m})}{h_r\Sigma_{tr}^2}\{2\mu_x^m[\exp(\frac{h_r\Sigma_{tr}}{2\mu_x^m})-1]^2 + h_r\Sigma_{tr}[\exp(\frac{h_r\Sigma_{tr}}{\mu_x^m})-1]\}$$

$$G_{00}^{x,m} = \frac{\exp(-\frac{h_r\Sigma_{tr}}{\mu_x^m})}{6h_r^2\Sigma_{tr}^3}\{-8(\mu_x^m)^2[1-2\exp(\frac{h_r\Sigma_{tr}}{2\mu_x^m}) + \exp(\frac{3h_r\Sigma_{tr}}{2\mu_x^m})] + 4h_r\mu_x^m\Sigma_{tr}[1-2\exp(\frac{h_r\Sigma_{tr}}{\mu_x^m}) + 2\exp(\frac{3h_r\Sigma_{tr}}{2\mu_x^m})] + 3h_r^2\Sigma_{tr}^2\exp(\frac{h_r\Sigma_{tr}}{\mu_x^m})\}$$

Figure 16 presents the function $\frac{1}{\alpha_x^m}$ , computed for a range of $\mu_x^m$ and $\Sigma_{tr}$ for $h_r$ =11.56 cm. It can be noticed that the dependency of $\frac{1}{\alpha_x^m}$ on $\Sigma_{tr}$ is more significant for the $\Sigma_{tr}$<0.3 cm$^{-1}$, that corresponds to the $\Sigma_{tr}$ in the fast energy-groups.

Equation (3) implies that the neutron leakage would be preserved, if $\gamma$ is selected such that $\Sigma_{tr}^{\gamma}$ is in good agreement with the functions $\frac{1}{\alpha_k^m}$ .

The functions $\Sigma_{tr}^{\gamma}$ for $\gamma = -1$ and $\gamma = -1/2$ have been compared with the function $\frac{1}{\alpha_x^m}$ , computed for $\mu_x^m$=0.9 (Figure 17). It can be noticed that the function $1/\sqrt{\Sigma_{tr}}$ is in better agreement with $\frac{1}{\alpha_x^m}$ than the function $1/\Sigma_{tr}$. The differences between $1/\sqrt{\Sigma_{tr}}$ and the function $1/\Sigma_{tr}$ are more significant in the regions of the smaller $\Sigma_{tr}$ (higher energy groups). It implies that the condensation of the transport XS by preserving $\Phi/\sqrt{\Sigma_{tr}}$ can provide better preservation of the neutron leakage especially in the fast energy groups than the conventional current-weighted method in the NEFD method of the code NSHEX.

The new weighting functions (4) that has been applied for the collapsing of the transport XS by the CCM have the feature to preserve $\frac{\Phi}{\sqrt{\Sigma_{tr,G}}}$ ,

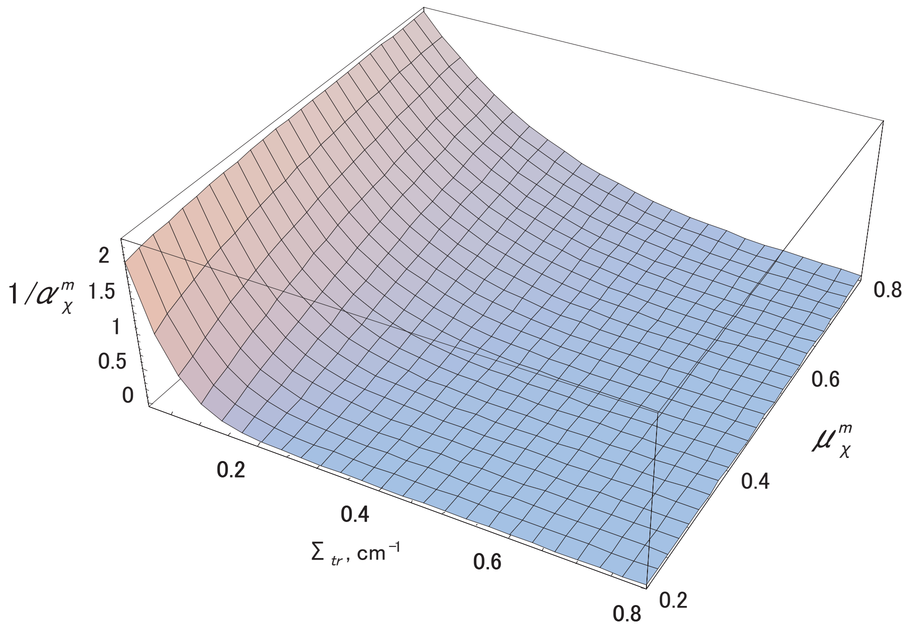


**Fig. 16 The dependency of the functions $\frac{1}{\alpha_x^m}$ on $\Sigma_{tr}$ and $\mu_x^m$ .**

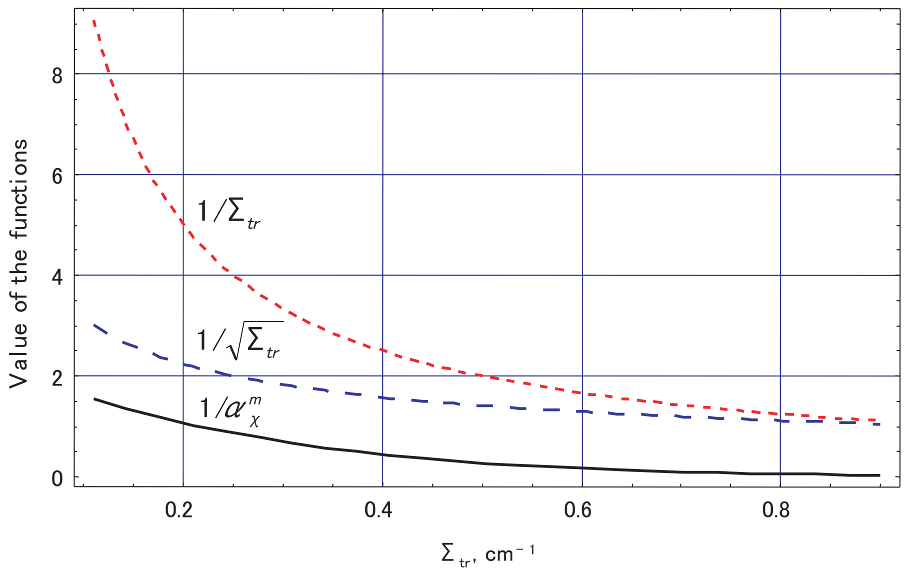


**Fig. 17 Comparison of the functions 1/ $\Sigma_{tr}$ and $1/\sqrt{\Sigma_{tr}}$ with $\frac{1}{\alpha_x^m}$ dependencies on the transport XS.**

which implies the preservation of the neutron current independent on the energy group approximations by selecting $\gamma$ of $\Sigma_{tr}^{\gamma}$ in good agreement with the function $\frac{1}{\alpha_k^m}$ , based on the above-mentioned discussions:

$$\sqrt{\Sigma_{tr,G}} = \frac{\sum_{g\in G} \sqrt{\Sigma_{tr,g}}\ \Phi_g / \sqrt{\Sigma_{tr,g}}}{\sum_{g\in G} \Phi_g / \sqrt{\Sigma_{tr,g}}} = \frac{\sum_{g\in G} \Phi_g}{\sum_{g\in G} \Phi_g / \sqrt{\Sigma_{tr,g}}}$$

$$\rightarrow \frac{1}{\sqrt{\Sigma_{tr,G}}} = \frac{\sum_{g\in G} \frac{1}{\sqrt{\Sigma_{tr,g}}} \Phi_g}{\sum_{g\in G} \Phi_g} \qquad (13)$$

This can be approximately given by substituting

$\gamma = -1/2$ into the equation (3).

## 7. Conclusions

The problem with the significant energy-group approximation effect in the few-group criticality analysis by the code NSHEX has been resolved by introducing of a collapsing algorithm for the transport XS by new weighting functions.

All numerical tests that have been conducted based on variety of FBR MONJU cores, confirmed the advantage of the new collapsing algorithm in comparison with the conventional current-weighted method. The energy-group collapsing effect of the effective multiplication factor has been reduced to negligibly small values. The spatial distribution of the fast flux has been significantly improved and has been found to be in better agreement with the 70 energy-group distribution. By analyzing the NEFD method of the code NSHEX in detail, it has been confirmed that the new weighting functions are in good agreement with the specific functions that are used in the code NSHEX in the simulation of the neutron leakage.

According to these results, the new collapsing algorithm can be recommended for application in the XS processing for the few-energy-group analyses by the code NSHEX instead of the conventional current-weighted method. Moreover, it should be noted that this collapsing algorithm could be applicable for the improvement of the energy-group collapsing effect of the nodal method transport calculation codes, which incorporate some intra-node flux distribution approximation. The transport XS collapsing algorithm should be carefully investigated and examined, especially for the nodal method transport codes, while they offer efficient resource saving for calculations.

## Acknowledgements

Dr. Galina Todorova would like to express her gratitude to Japan Society for the Promotion of Science (JSPS) that sponsors her research in Japan.

## References

1 ) S. Sawada, T. Suzuki, *et al*.,“ Reactivity characteristics evaluations of the initial core of MONJU, ”*PHYSOR 96*, Mito, Japan, Sept. 16-20, 1996, Vol.3, pp.E76-E85, (1996)

2 ) S. Usami, T. Suzuki, *et al*.,“ Evaluation of the FBR MONJU Core Breeding Ratio and the Power Distribution from the Reaction Rate Distribution Measurement, ”*PHYSOR 96*, Mito, Japan, Sept. 16-20, 1996, Vol.3, pp.E86-E95, (1996)

3 ) K. Sasaki, T. Suzuki, *et al*.,“ Operational Results of the Prototype FBR Monju - Analysis of Measured Reactivity Characteristics Using JENDL-3.2, ”*Trans. ENC'98*, Nice, France, Oct. 25-28, 1998, Vol.IV, pp.110-118, (1998)

4 ) A. Kitano, H. Teruyama, *et al*., “ Development of Monju Easy-to-Introduce System for Total Evaluation of Reactor Core, ”JNC TW4418 2001-002, Japan Nuclear Cycle Development Institute (JNC), (2002) [in Japanese].

5 ) H. Ikeda and T. Takeda,“ A New Nodal Sn Transport Method for Three-Dimensional Hexagonal Geometry, ”*J. Nucl. Sci. Technol*., 31[6], 497 (1994)

6 ) J. Ishibashi, Y. Morohashi, *et al*.,“ A study on correction factors for the Monju initial critical core criticality analysis, ”*Proc. 2002 Fall Meeting of the Atomic Energy Society of Japan*, Iwaki, Japan, Sept. 14-16, 2002, p. 407 (M31), (2002), [in Japanese].

7 ) J. Y. Doriath, *et al*.,“ ERANOS1: The Advanced European System of Codes for Reactor Physics Calculation, ”Int. Conf. on Mathematical Methods and Super Computing in Nuclear Applications, Karlsruhe, Germany (Apr. 1993)

8 ) K. Sugino,“ A new method of treating radial leakage in nodal $S_N$ transport calculation for hexagonal geometry, ”*Proc. PHYSOR'96*, Mito, Japan, Sept. 16-20, 1996, Vol.1, p. A-153, (1996)

9 ) K. Sugino and T. Takeda,“ An improvement of the transverse leakage treatment for the nodal $S_N$ transport calculation method in hexagonal-Z geometry, ”*J. Nucl. Sci. Technol*., 33[8], p.620-627 (1996)

10) T. Takeda and H. Ikeda,“ Three-Dimensional Neutron Transport Benchmarks, ”NEACRP-L-330, (1991)

11) T. Mori and M. Nakagawa,“ MVP/GMVP: General purpose Monte Carlo codes for neutron and photon transport calculations based on continuous energy and multigroup methods, ”JAERI-Data/Code 94-007, Japan Atomic Energy Research Institute (JAERI), (1994) [in Japanese].

12) G. Todorova, H. Nishi, J. Ishibashi,“ Transport Criticality Analysis of FBR MONJU Initial Critical Core in Whole Core Simulation by NSHEX and GMVP, ”*J. Nucl. Sci. Technol*., 41[4], pp. 493-501, (2004)

13) G. Todorova, H. Nishi, J. Ishibashi,“ A study on En-

技術報告

ergy Group Dependency of Transport Effect in FBR MONJU Initial Critical Core Criticality Analysis," Proc. 2003 Fall Meeting of the Atomic Energy Society of Japan, Shizuoka, Japan, Sept. 24-26, 2003, pp. 301 (E22), (2003)

14) G. Todorova, H. Nishi, J. Ishibashi, "Transport Criticality Analysis for FBR MONJU Initial Critical Core in Whole Core Simulation by NSHEX and GMVP," *JNC Technical Review*, 22[2004.3], pp. 1-10, (2004)

15) G. Todorova, H. Nishi, J. Ishibashi, "A Study on the Effect of the Cross-Sections Collapsing Method in FBR MONJU Criticality Analysis by the Transport Codes NSHEX and GMVP, "Proc. 2004 Annual Meeting of the Atomic Energy Society of Japan, Okayama, Japan, March. 29-31, 2004, pp. 490 (O55), (2004)

16) G. Todorova, H. Nishi, J. Ishibashi, "Method for the Macroscopic Transport Cross-Sections for Criticality Analyses of FBR MONJU by the Code NSHEX," *J. Nucl. Sci. Technol*., 41[12], pp. 1237-1244, (2004)

17) T. Nakagawa, T. Kawano, et al., "Japanese evaluated nuclear data library Version 3 Revision-2: JENDL 3.2," *J. Nucl. Sci. Technol*., 32[12], pp.1259-1271 (1995)

18) M. Nakagawa and K. Tsuchihashi, "SLAROM: a code for cell homogenization calculation of fast reactor, "JAERI 1294, (JAERI), (1984)

19) M. Nakagawa, J. Abe, W. Sato, "Code System for Fast Reactor Neutronics Analysis, "JAERI-M 83-066, (JAERI), (1982).

20) T. B. Fowler, D. R. Vondy, G. W. Cunningham "Nuclear reactor analysis code: CITATION, "ORNL-TM-2496, Rev.2, Oak Ridge National Laboratory (1971).

21) A. E. Waltar and A. B. Reynols, *Fast Breeder Reactors*, Pergamon Press (1981)